Properties of the Cysteine Residues and Iron−Sulfur Cluster of the Assimilatory 5′-Adenylyl Sulfate Reductase from *Pseudomonas aeruginosa*†

Sung-Kun Kim,‡ Afroza Rahman,§,|| Julie-Ann Bick,||,+ Richard C. Conover,# Michael K. Johnson,# Jeremy T. Mason,‡ Masakazu Hirasawa,‡ Thomas Leustek,|| and David B. Knaff*,‡,@

Department of Chemistry and Biochemistry, Center for Biotechnology and Genomics, Texas Tech University, Lubbock, Texas 79409-1061, Biotechnology Center for Agricultural and the Environment, Department of Plant Biology and Pathology, Rutgers University, New Brunswick, New Jersey 08901-8520, and Department of Chemistry and Center for Metalloenzyme Studies, University of Georgia, Athens, Georgia 30602

Received June 8, 2004; Revised Manuscript Received August 2, 2004

ABSTRACT: APS reductase from *Pseudomonas aeruginosa* has been shown to contain a [4Fe−4S] cluster. Thiol determinations and site-directed mutagenesis studies indicate that the single [4Fe−4S] cluster contains only three cysteine ligands, instead of the more typical arrangement in which clusters are bound to the protein by four cysteines. Resonance Raman studies in the Fe−S stretching region are also consistent with the presence of a redox-inert $[4Fe-4S]^{2+}$ cluster with three cysteinate ligands and indicate that the fourth ligand is likely to be an oxygen-containing species. This conclusion is supported by resonance Raman and electron paramagnetic resonance (EPR) evidence for near stoichiometric conversion of the cluster to a $[3Fe-4S]^{+}$ form by treatment with a 3-fold excess of ferricyanide. Site-directed mutagenesis experiments have identified Cys139, Cys228, and Cys231 as ligands to the cluster. The remaining two cysteines present in the enzyme, Cys140 and Cys256, form a redox-active disulfide/dithiol couple (E_m = −300 mV at pH 7.0) that appears to play a role in the catalytic mechanism of the enzyme.

Sulfate assimilating bacteria are capable of reducing sulfur from the +6 oxidation state found in sulfate to the −2 oxidation state required for cysteine and methionine biosynthesis. The pathway of sulfate assimilation was first characterized in *Escherichia coli*, where six catalytic steps were genetically defined (*1*). One of the reactions is mediated by the *cysH* gene product, 3′-phosphoadenylyl sulfate (PAPS) reductase, an enzyme that catalyzes the formation of sulfite from PAPS using thioredoxin as an electron donor. Recent evidence indicates that a related, but structurally and catalytically distinct form of CysH that uses 5′-adenylyl sulfate (APS) as the substrate instead of PAPS, exists in genera from all the major eubacterial divisions and in photosynthetic eukaryotes (*2*−*7*). The phylogenetic distribution of these two types of sulfonucleotide reductases suggests that the PAPS-dependent form evolved from the APS-dependent form (*8*).

The assimilatory PAPS and APS reductases share significant amino acid sequence homology (Figure 1). In particular, both contain a motif (KRT)ECG(LI)H that includes a catalytically active Cys residue (*9*, *10*). In addition to the catalytic domain, the APS reductases contain two motifs, CCXXRKXXPL and SXGCXXCT, that are not found in the PAPS reductases (Figure 1). Three of the four Cys residues found in these domains appear to be ligands for a $[4Fe-4S]^{2+}$ cluster (*8*). The APS reductase motifs and the iron−sulfur center have been proposed to define the specificity of the enzymes for APS (*7*, *8*). The *cysH* enzyme from *Bacillus subtilis*, which contains a $[4Fe-4S]^{2+}$ cluster and is of the APS reductase type, has recently been shown to exhibit a dual substrate specificity for APS and PAPS (*11*). Although this finding does not directly contradict the idea that the iron−sulfur center is a determinant of the specificity for APS as substrate, it does highlight the fact that the functions of the iron−sulfur center and of the conserved APS reductase domains have not yet been elucidated.

The three-dimensional structure of *E. coli* PAPS reductase is known, and its catalytic mechanism has been explored through kinetic experiments (*9*, *12*). A two-step cycle (ping−pong mechanism) was proposed in which the homodimeric enzyme, linked by an intermolecular disulfide bond, is reduced to two monomers by thioredoxin. The monomeric, reduced form of the enzyme then carries out a two-electron reduction of PAPS to produce sulfite and adenosine 3′,5′-bisphosphate (PAP), in the process regenerating the oxidized homodimeric enzyme. The Cys residue of the (KRT)ECG(LI)H motif was proposed to function as the catalytic nucleophile. Mutation of this Cys inactivates PAPS reductase (*9*).

The reaction catalyzed by APS reductase, using thioredoxin as an electron donor is

$$\text{APS} + \text{reduced thioredoxin} \rightarrow \text{sulfite} + \text{AMP} + \text{oxidized thioredoxin}$$

† Supported by grant from the U.S. Department of Agriculture (2002-35318-12503 to T.L. and D.B.K.) and from the National Institutes of Health (GM62542 to M.K.J.).

* To whom correspondence should be addressed. Phone: (806) 742-0288; fax: (806) 742-2025; e-mail: knaff@ttu.edu.

‡ Department of Chemistry and Biochemistry, Texas Tech University.

§ Current address: Sun Health Research Institute, 10510 W. Santa Fe Dr., Sun City, AZ 85351.

|| Rutgers University.

+ Current address: Aventis, 1041 Route 202-206, P.O. Box 6800, Bridgewater, NJ 08807-0800.

University of Georgia.

@ Center for Biotechnology and Genomics, Texas Tech University.

10.1021/bi048811t CCC: $27.50
Published on Web 10/02/2004

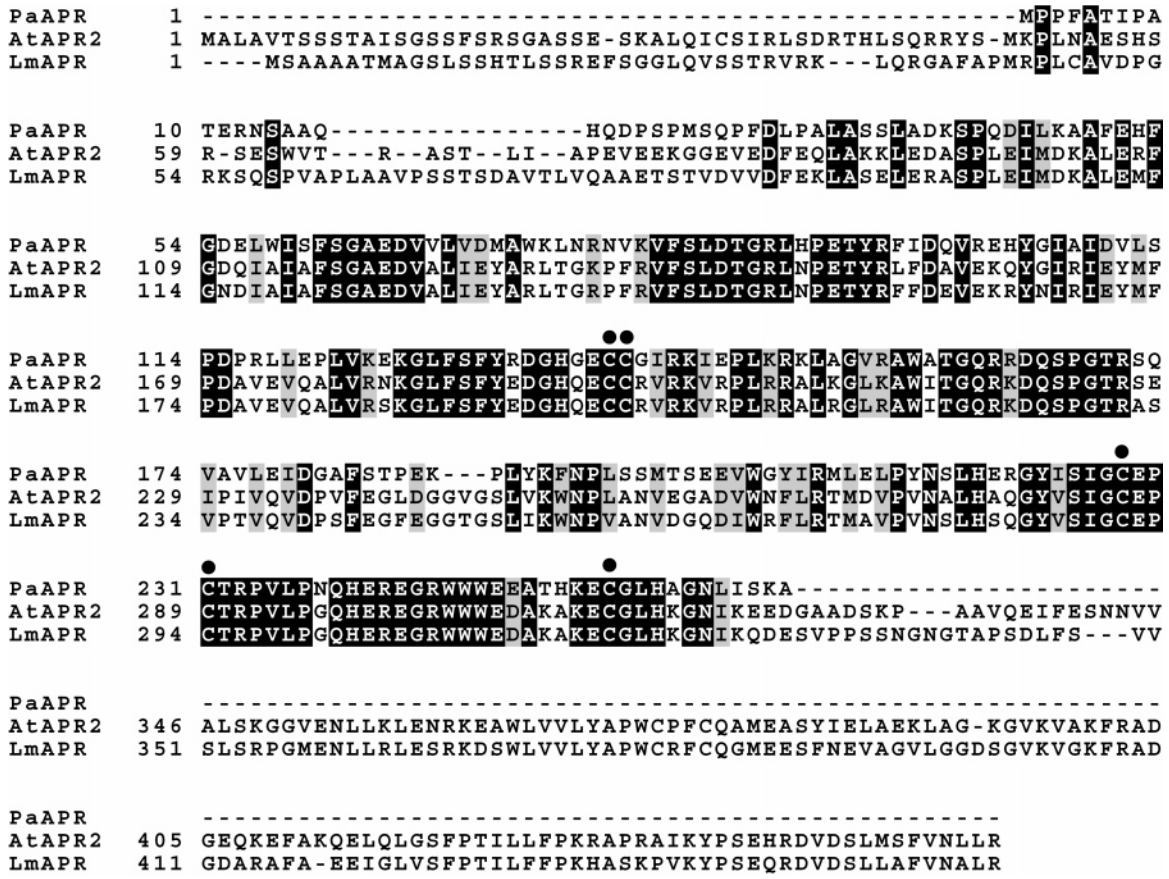

FIGURE 1: Sequence alignment of APRs. PaAPR, AtAPR2, and LmAPR were aligned using ClustalW. The alignment was shaded using BoxShade. Amino acid residues conserved in all three sequences are black, and conservative substitutions are gray. The Cys residues referred to in the text are indicated with a dot above the PaAPR sequence.

In this reaction, APS reductase catalyzes the two-electron reduction of APS, producing sulfite. Whether APS reductases function via a mechanism similar to PAPS reductases is not clear. Kinetic analysis of the APS reductase of *P. aeruginosa* (hereafter abbreviated as PaAPR)[1] showed that its catalytic cycle also involves a ping−pong reaction mechanism (*5*). Mutation of the Cys residue in the (KRT)ECG(LI)H motif inactivated one of the APS reductase isoforms (AtAPR2) present in chloroplasts of the plant *Arabidopsis thaliana* (*10*). Furthermore, this Cys residue was reported to form a sulfonate bond (with the sulfite originating from APS) that could be subsequently reduced by thioredoxin (*10*), suggesting that the catalytic mechanism of APS reductases might differ somewhat from the catalytic mechanism of PAPS reductase. In this context, it should be noted that bacterial and plant APS reductases differ in structure, with the plant enzymes containing, in addition to an APS reductase domain, a C-terminal domain that is functionally similar in many ways to glutaredoxin (*13*). As bacterial APS reductases, such as the *P. aeruginosa* enzyme, do not contain the glutaredoxin-like domain found in the plant enzymes, it is possible that the mechanisms of two types of APS reductases differ.

The present investigation was undertaken to lay the foundation for mechanistic investigations of PaAPR by characterizing the iron−sulfur prosthetic group present in the enzyme and the oxidation−reduction and some chemical reactivity properties of the five cysteine residues known to be present in the enzyme.

MATERIALS AND METHODS

Biochemical Methods. A culture of *E. coli* BL21 (DE3) pLysS harboring the plasmid pET-PaAPR (*5*) was grown in LB medium containing 50 μg/mL kanamycin and 34 μg/mL chloramphenicol at 37 °C to an optical density at 600 nm of 0.6. IPTG (isopropyl-β-d-thioglactopyranside) was then added, to a final concentration of 1 mM, and growth was continued for 4 h in LB medium at 30 °C. Cells were then harvested by centrifugation, resuspended in 20 mM Tris-HCl buffer (pH 8.0), passed twice through a French-Press at 18 000 psi, and centrifuged. The supernatant was filtered through 0.45 μm pore-size membrane and applied to a Ni^{2+} affinity column (HiTrap Chelating HP, obtained from Amersham Biosciences) incorporated into a BioCAD perfusion chromatography system (PerSeptive BioSciences). The column was washed with 200 mL of 20 mM Tris-HCl buffer (pH 8.0) containing 500 mM NaCl (buffer A), supplemented with 10 mM imidazole, followed by being washed with 20 mL of buffer A containing 125 mM imidazole. The His-tagged PaAPR was then eluted with buffer A containing 250 mM imidazole. All solutions used for the Ni^{2+} affinity chromatography were degassed and purged with helium gas.

[1] Abbreviations: AtAPR, any of the three isoforms of *Arabidopsis thaliana* APS reductase; AtAPR2, *A. thaliana* APS reductase encoded by locus At1g62182; LmAPR, *Lemna minor* APS reductase; DTT, dithiothreitol; EPR, electron paramagnetic resonance; mBBr, monobromobimane; PaAPR, *Pseudomonas aeruginosa* APS reductase; PAGE, polyacrylamide gel electrophoresis; RR, Resonance Raman; SDS, sodium dodecyl sulfate; VTMCD, variable-temperature magnetic circular dichroism.

The imidazole was removed by buffer exchange against 20 mM Tris-HCl buffer (pH 8.0) containing 100 mM sodium sulfate, using an Amicon YM10 membrane. The use of oxygen-free buffers during chromatography prevented partial loss of the iron−sulfur cluster of PaAPR during Ni^{2+} affinity chromatography.

Both the purity of PaAPR and its molecular mass were estimated by polyacrylamide gel electrophoresis (PAGE) on 10% gels, in the presence of sodium dodecyl sulfate (SDS), carried out as described by Sambrook et al. (*14*). Protein purity and molecular mass were also measured by MALDI-TOF mass spectrometry, using a PerSeptive Biosystems Inc. Voyager DE time-of-flight mass spectrometer operating in the linear mode. The instrument has a 1.2 m flight tube and an adjustable accelerating voltage (with a 25 kV maximum in the delayed extraction mode). Radiation from a nitrogen laser (337 nm, 3 ns pulse width) was used to desorb ions from the target, and data were collected and accumulated from between 128 and 256 laser pulses. The matrix solution used for sample preparation was a saturated sinapinic acid solution in a solvent system consisting of 1:1 mixture of acetonitrile and water containing 0.1% (v/v) trifluoroacetic acid (TFA). External calibration was carried out using chicken egg lysozyme *c* ($[M + H]^+$; 14306.1) and bovine serum albumin ($[M + H]^+$; 66431.0) as standards. N-terminal amino acid sequencing was determined in the Biotechnology Core Facility at Texas Tech University by automated, repetitive Edman degradation using a Porton 2020 sequencer.

PaAPR enzymatic activity was assayed essentially as described by Bick et al. (*5*). The 100 μL reaction contained 10 μmol of TrisHCl (pH 8.0), 0.1 μmol of EDTA, 0.5 μmol of DTT, 10 nmol of *E. coli* thioredoxin (Promega Inc. stock #Z7051), and 5 nmol of [^{35}S]APS (500 Bq $nmol^{-1}$). The reaction was incubated at 30 °C for 20 min.

The thiol content of oxidized and reduced samples of PaAPR was determined using DTNB (5,5′-dithiobis(2-nitorbenzoic acid), as described previously (*15*). Oxidized and reduced samples of PaAPR were prepared by incubating the enzyme with either oxidized DTT or reduced DTT, respectively, at a concentration of 5 mM for 2 h. Reduced DTT was then removed by gel filtration on a Sephadex G-10 column. Total free thiols were titrated with DTNB in the presence of 2% (w/v) SDS in 100 mM Tris-HCl, pH 8.0, and surface-exposed cysteines in 100 mM Tris-HCl, pH 8.0, in the absence of SDS. Release of TNB^- was monitored at 412 nm, and its concentration was calculated with a molar absorbency of 13 600 M^{-1} cm^{-1} (*16*). Total iron content was determined according to the procedure of Massey (*17*), using ferric ammonium sulfate as a standard. Acid-labile sulfide was determined by the procedure described in ref *18*. The absorbance at 670 nm of the preparations was determined after 20 min to allow color development.

Oxidation−reduction titrations of disulfide/dithiol redox couples in PaAPR were carried out as described previously (*19*, *20*) using either thiol labeling with monobromobimane (mBBr), followed by quantitation of the fluorescence arising from the mBBr adducts of the protein, or the intrinsic tryptophan fluorescence of the protein to monitor the redox state of PaAPR cysteines. The titration data all gave excellent fits to a single-component Nernst equation for a two-electron component. E_m values were independent of redox equilibration time and of the total DTT concentration present in the redox equilibration buffer. Identical titration curves were observed regardless of whether they were carried out under ambient oxygen concentrations or under an argon atmosphere. The experimental uncertainties for all values reported next, regardless of the parameter measured (designated by a ± symbol) represent the average deviations.

Spectroscopic Methods: UV−visible absorption spectra were recorded using either Shimadzu UV-3101PC or Shimadzu UV-2401PC spectrophotometers. X-band (~9.6 GHz) electron paramagnetic resonance (EPR) spectra were recorded on a Bruker ESP-300E EPR spectrometer equipped with an ER-4116 dual-mode cavity and an Oxford Instruments ESR-9 flow cryostat. Resonances were quantified under nonsaturating conditions using a 1 mM Cu-EDTA standard. Resonance Raman (RR) spectra were recorded using an Instruments SA U1000 spectrometer fitted with a cooled RCA 31034 photomultiplier tube with 90° scattering geometry. Spectra were recorded digitally using photon-counting electronics, and improvements in signal-to-noise were achieved by averaging multiple scans. Band positions were calibrated using the excitation frequency and are accurate to ±1 cm^{-1}. Lines from a Coherent Sabre 10-W Argon Ion Laser were used for excitation, and plasma lines were removed using a Pellin Broca prism premonochromator. Scattering was collected from the surface of a frozen droplet of sample at 17 K using a custom designed anaerobic sample cell (*21*) attached to the coldfinger of an Air Products Displex model CSA-202E closed cycle refrigerator. Bands originating from lattice modes of ice and a linear ramp fluorescent background have been subtracted from each spectrum shown in this work. Variable-temperature magnetic circular dichroism (VTMCD) measurements were carried out with an Oxford Instruments Spectromag 4000 split-coil superconducting magnet mated to a Jasco J730 spectropolarimeter using the published protocols (*22*, *23*). Variable-field, variable-temperature MCD saturation magnetization data were collected by monitoring the MCD intensity at fixed temperatures as a function of applied magnetic field.

RESULTS

The construct used to express the wild-type form of PaAPR in *E. coli* was designed with a six-histidine extension at the N-terminus to allow facile purification of the enzyme from soluble *E. coli* extracts using a Ni^{2+} affinity column. SDS−PAGE analysis of freshly prepared samples of the His-tagged, recombinant PaAPR showed a single major Coomassie-staining band with an apparent molecular mass of 35 kDa and a much fainter band with an apparent molecular mass of 70 kDa, consistent with the presence of a small amount of homodimer. It should be mentioned that SDS−PAGE analysis of His-tagged, recombinant PaAPR, purified by conventional Ni^{2+} affinity chromatography under aerobic conditions, instead of being purified rapidly under a He atmosphere (as described previously in the Materials and Methods), showed considerably larger amounts of PaAPR homodimer and also contained Coomassie-staining bands that are likely to arise from higher molecular mass homooligomers. Gels and N-terminal amino acid sequencing of freshly prepared samples of PaPAR (purified as described in the Materials and Methods) indicated that the material was at least 95% pure. The amino acid sequence for the N-terminal

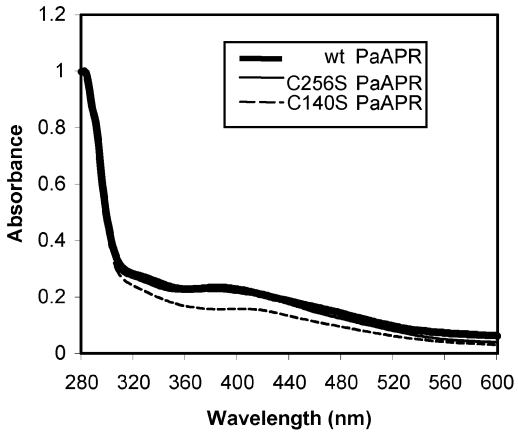

FIGURE 2: Optical spectra of purified wild-type PaAPR and its variants. Wild-type PaAPR and C256S variant of PaAPR contains 30 mM Tris-HCl (pH 8.0) with 100 mM sodium sulfate; C140S variant of PaAPR contains 130 mM Tris-HCl (pH 8.0) with 100 mM sodium sulfate and 10 mM 2-mercaptoethanol. Spectra were normalized to equal A_{280}.

region of the protein, determined by 17 cycles of repetitive automated Edman degradation, was MHHHHHHSSGLV-PRGSG, exactly that expected from the known sequence of the enzyme with its added His-tag. MALDI-TOF mass spectrometry of freshly prepared samples of PaAPR showed a single major component with a molecular mass of 35432 ± 18 Da, in good agreement with the calculated mass of 35443 Da for the His-tagged monomer. SDS−PAGE analysis of recombinant, wild-type PaAPR that had been stored for some time after elution from the Ni^{2+} affinity column showed two Coomassie-staining bands, one with an apparent molecular mass of 35 kDa and a second band with a lower molecular mass. Amino acid sequencing of this second band showed an N-terminal sequence of SQPFDLPALASS-LADKSPQ, indicating that the lower molecular mass species is PaAPR that has lost the first 71 amino acids (see sequence in Figure 1) due to an as-yet uncharacterized proteolysis reaction.

Figure 2 shows the absorbance spectrum of the PaAPR in the visible and near-ultraviolet regions of the spectrum. The spectrum, which contains a peak at 281 nm and a broad absorbance feature centered at 385 nm, is similar to those reported previously for PaAPR (*8*) and for three other APS reductases reported to contain a single [4Fe−4S] cluster (*24*), the *B. subtilis* APS/PAPS reductase (*11*), the *L. minor* APS reductase (LmAPR), and one of the three APS reductases (AtAPR2) found in chloroplasts of *Arabidopsis thaliana* (*24*). Non-heme iron and acid-labile sulfide analyses of freshly prepared PaAPR indicated the presence of 3.96 ± 0.04 mol of iron and 3.65 ± 0.07 mol of sulfide per mole of enzyme, consistent with the presence of a single [4Fe−4S] cluster per enzyme monomer (Table 1). A similar non-heme iron content was previously reported for PaAPR, but no acid-labile sulfide analyses were reported in the earlier study (*8*). An earlier report of the acid-labile sulfide analysis of the LmAPR showed only 2.9 mol of sulfide per mol of enzyme (*24*).

Mössbauer spectroscopy of PaAPR (*8*) and of the LmAPR enzyme provided evidence suggesting that the [4Fe−4S] cluster in both of the two higher plant APS reductases is ligated to the protein by only three cysteine ligands, instead

Table 1: Analysis of Iron and Acid-Labile Sulfide Contents for Wild-Type PaAPR and Its Variants

	iron content (nmol/nmol of protein)	sulfide content (nmol/ nmol of protein)
wild-type	3.96 ± 0.04	3.65 ± 0.07
C139S	0.16 ± 0.06	none
C140S	3.20 ± 0.32	2.31 ± 0.19
C228S	0.07 ± 0.04	none
C231S	0.26 ± 0.07	none
C256S	3.57 ± 0.11	3.22 ± 0.05

of the four cysteine ligands more commonly found in most [4Fe−4S] cluster-containing proteins (*24*). Independent chemical evidence for a [4Fe−4S] cluster ligated by three cysteine ligands in PaAPR was sought by measurement of the thiol content. The number of cysteine thiol groups was quantitated in samples of the cluster-replete recombinant enzyme that had been treated with dithiothreitol (DTT) and in DTT-reduced samples from which the iron−sulfur cluster had first been removed by denaturation with sodium dodecyl sulfate (SDS). The thiol content of the reduced recombinant enzyme (i.e., the cluster-replete form of the enzyme), as determined using the DTNB method, was 2.16 ± 0.37 mol per mol of enzyme, while that of the reduced, cluster-free enzyme was 5.03 ± 0.09 mol per mol of enzyme. The difference between these two values (i.e., 2.87) is consistent (within the experimental uncertainties of the measurements) with the presence of three cysteine ligands to the iron−sulfur cluster but is not consistent with the presence of four cysteine ligands to the cluster. The as-isolated, cluster-replete PaAPR (i.e., protein to which neither reductant nor oxidant had been added) contained 0.37 mol of thiol per mol of enzyme, indicating that a substantial portion of the two cysteines that do not serve as cluster ligands has formed an intramolecular disulfide.

Spectroscopic evidence for the presence of a $[4Fe-4S]^{2+}$ cluster with three cysteine ligands in PaAPR was provided by resonance Raman (RR) studies using 457.9 and 488.0 nm excitation. The low-temperature RR spectrum of wild-type PaAPR in the Fe−S stretching region obtained with 488.0 nm excitation is shown in Figure 3a. The spectrum shown is for a sample in the presence of reduced DTT. However, identical spectra, albeit with lower signal-to-noise, were obtained in the absence of DTT (data not shown). DTT appears to stabilize the Fe−S cluster in PaAPR, particularly at the high concentrations required for RR studies (1−3 mM), and the poor quality spectra observed in the absence of DTT are attributed to partial loss of clusters during concentration. The RR spectrum of PaAPR is uniquely indicative of a $[4Fe-4S]^{2+}$ cluster (*25*), and the frequencies and relative intensities of Fe−S stretching modes are most similar to those observed for the $[4Fe-4S]^{2+}$ center in mitochondrial aconitase (*26*), which has three cysteinate and one water-derived ligand. Hence, the Fe−S stretching modes of the $[4Fe-4S]^{2+}$ cluster in PaAPR can be assigned by direct analogy to aconitase, for which detailed assignments are available based on normal mode calculations and ^{34}S isotope shifts (see Table 2). The frequency of the totally symmetric breathing mode of the [4Fe−4S] cube has been found to be a useful indicator of cluster ligation, and the frequency of this mode in PaAPR, 339 cm^{-1}, lies in the range established for $[4Fe-4S]^{2+}$ clusters with three cysteinate ligands and an oxygenic ligand at a unique Fe site (i.e., 338−343 cm^{-1} (*27*−*29*)).

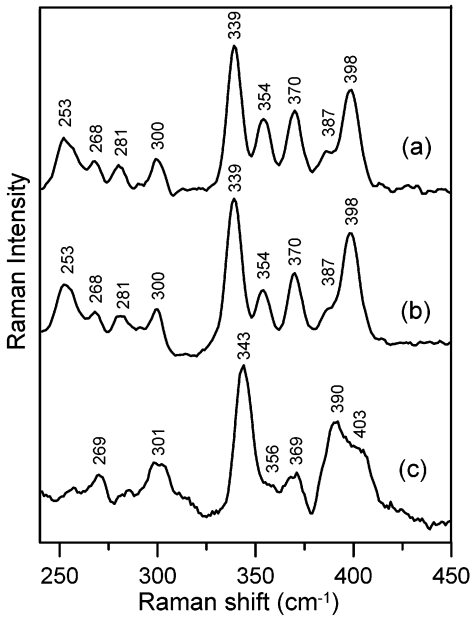

FIGURE 3: Resonance Raman spectra of *P. aeruginosa* APS reductase: (a) wild-type PaAPR; (b) C256S variant of PaAPR; (c) wild-type PaAPR in the presence of a 3-fold stoichiometric excess of potassium ferricyanide. The spectra were recorded at 17 K using 488.0 nm excitation (200 mW of laser power at the sample), with samples that were 1.7 mM in PaAPR and DTT. Each spectrum is sum of 100 scans, with each scan involving photon counting for 1 s at 1 cm^{-1} increments with 8 cm^{-1} spectral resolution.

Table 2: Vibrational Frequencies (cm^{-1}) and Assignments for the Fe−S Stretching Modes of the $[4Fe-4S]^{2+}$ and $[3Fe-4S]^{+}$ Centers in Beef Heart Aconitase and *P. Aeruginosa* APS Reductase

assigment, C_{3v} symmetry	aconitase[a]	PaAPR
Predominantly Fe−S^t stretching of $[4Fe-4S]^{2+}$ centers		
A_1	372(2)	370
E	352(2), 360(1)	354
Predominantly Fe−S^b stretching of $[4Fe-4S]^{2+}$ centers		
A_1	392(4)	398
E		387[b]
A_1	339(6)	339
A_1	299(3)	300
B_1	287(5)	287[b]
E	275(4)	281
A_2	269(3)	268
A_1, E	255(5)	253
Predominantly Fe−S^t stretching of $[3Fe-4S]^{+}$ centers		
A_1	372(1)	369
E	359(0)	356
Predominantly Fe−S^b stretching of $[3Fe-4S]^{+}$ centers		
A_1	400(4)	403
E		390
A_1	342(8)	343
A_2, E	293(4)	301
E	264(5)	269

[a] Taken from ref *26*, with $^{34}S^b$downshifts in parentheses. [b] More clearly observed with 457.9 nm excitation.

PaAPR, as-isolated, exhibited a weak, fast-relaxing, nearly isotropic EPR signal centered near $g = 2.01$ that accounts for less than 0.02 spins per mol of enzyme. Similar trace EPR signals accounting for ≤0.1% of the chemically determined Fe were reported in as-isolated samples of the recombinant forms of the APRs from two higher plants, *L. minor* and *A. thaliana*, and attributed to minor contributions from $S = 1/2$ $[3Fe-4S]^{+}$ clusters based on ^{57}Fe broadening

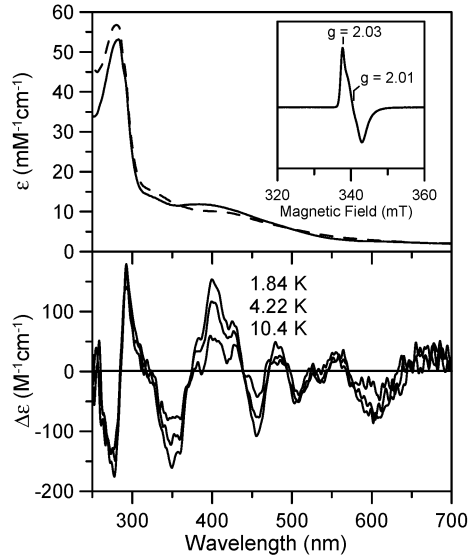

FIGURE 4: UV−vis absorption, VTMCD, and EPR spectra of ferricyanide-treated PaAPR. Upper panel: UV−vis absorption of 0.11 mM PaAPR in 100 mM Tris-HCl buffer, pH 8.0, with 100 mM NaCl, before (solid line) and after (broken line) addition of a 3-fold stoichiometric excess of potassium ferricyanide. Inset shows the EPR spectrum of the ferricyanide-treated sample recorded at 12 K, with a microwave power of 1 mW, using 0.63 mT modulation amplitude and 9.59 GHz microwave frequency. Lower panel: VTMCD spectra of ferricyanide-treated PaAPR. Spectra recorded with an applied field of 6 T at 1.84, 4.22, and 10.4 K. All bands increase in intensity with decreasing temperature. The sample used for VTMCD was the same as that used for the absorption and EPR studies except for the addition of 55% (v/v) ethylene glycol to facilitate glass formation on freezing.

(*24*). It was also reported that anaerobic reduction of *L. minor* and *A. thaliana* enzymes using sodium dithionite or photochemically using 5′-deazaflavin/oxalate photoreduction resulted in ~50% bleaching of the visible absorbance centered at 400 nm (*24*). However, this bleaching was not reversed by the addition of O_2, and no EPR signals characteristic of a reduced $[4Fe-4S]^{1+}$ cluster were observed with either the dithionite-reduced enzymes or the photoreduced plant enzymes (*24*). We have attempted to reduce the iron−sulfur cluster of PaAPR by a variety of techniques (by addition of sodium dithionite in the absence and presence of DTT, by addition of Ti(III) citrate, and by photoreduction using 5′-deazaflavin/oxalate), but, at most, only a very small bleaching (less than 5%) of the absorbance at 400 nm was observed. In addition, EPR and VTMCD spectra of the enzyme samples treated with these reductants showed no evidence for formation of $S = 1/2$ or 3/2 $[4Fe-4S]^{+}$ clusters.

To assess the possibility that the $S = 0$ $[4Fe-4S]^{2+}$ can be oxidized to a stable $S = 1/2$ $[4Fe-4S]^{3+}$ cluster, as in HiPIP-type [4Fe−4S] centers, excess ferricyanide was added to the enzyme. However, rather than resulting in the formation of a $[4Fe-4S]^{3+}$ cluster, EPR, UV−vis absorption, VTMCD, and RR studies all demonstrated that ferricyanide treatment resulted in the oxidative removal of one iron from the [4Fe−4S] cluster, to yield a $[3Fe-4S]^{+}$ cluster (see Figures 3 and 4). Optimal conversion was achieved using a 3-fold excess of ferricyanide, and the resulting sample exhibited a modified absorption spectrum with small increases between 300 and 350 nm and 500−650 nm and a small decrease between 350 and 500 nm and the appearance of an intense, fast relaxing, nearly isotropic EPR resonance

centered around $g = 2.01$, accounting for 0.7 spins per mol of enzyme. $[3Fe-4S]^+$ clusters invariably exhibit $S = 1/2$ ground states with EPR signals typically comprising a well-defined low-field component centered at $g = 2.03$ and poorly resolved high-field components as a result of microheterogeneity in the cluster structure (*30*). The nearly isotropic resonance observed in ferricyanide-treated PaAPR is most similar to that reported for the cubane-type $[3Fe-4S]^+$ cluster formed via oxidative degradation of the $[4Fe-4S]^{2+}$ clusters in aconitase (*26*). Confirmation that this resonance originates from a $S = 1/2$ $[3Fe-4S]^+$ cluster is provided by the characteristic pattern of temperature-dependent bands in the VTMCD spectrum (*30*). Figure 4 and MCD saturation magnetization data (not shown) indicate that all transitions originate from the EPR-active $S = 1/2$ ground state. The ferricyanide-induced changes in the RR spectrum (Figure 3c) are also indicative of near-complete cluster conversion to form a $[3Fe-4S]^+$ cluster. The Fe−S stretching frequencies and resonance enhancements are very similar to those reported and assigned for the $[3Fe-4S]^+$ cluster in aconitase (*26*), and the spectrum observed in PaAPR is assigned by direct analogy (see Table 2).

The ability to induce almost stoichiometric conversion of $[4Fe-4S]^{2+}$ clusters to $[3Fe-4S]^+$ clusters by incubating with ferricyanide appears to be a unifying attribute of $[4Fe-4S]^{2+}$ with three cysteinate ligands and oxygenic coordination at the removable Fe site (*30*). Hence, the near stoichiometric formation of a $[3Fe-4S]^+$ cluster in PaAPR provides additional support for the presence of only three cysteinate ligands to the $[4Fe-4S]^{2+}$ cluster. Attempts to purify the [3Fe−4S] cluster form of PaAPR for activity studies to address the catalytic role of the unique Fe site proved unsuccessful. Reconversion to a $[4Fe-4S]^{2+}$ cluster, together with significant cluster degradation, occurred on removal of excess ferricyanide under either aerobic or anaerobic conditions, even in the presence of EDTA. This appears to be a consequence of a high potential for the $[3Fe-4S]^{+,0}$ couple, such that it is only stable in the presence of ferricyanide, coupled with rapid and efficient Fe incorporation by the $[3Fe-4S]^0$ cluster. The latter process is invariably observed for [3Fe−4S] centers that are oxidation artifacts and often involves cluster cannibalization (*30*, *31*).

It was of obvious interest to determine which three of the five cysteines known to be present in PaAPR serve as iron−sulfur cluster ligands. Site-directed mutagenesis was carried out, and each of the five cysteine residues individually changed to serine. Figure 2 shows that the visible-region spectra of the C140S and the C256S variants of PaAPR both retain the features seen in the spectrum of the wild-type enzyme that arise from the [4Fe−4S] cluster (the C256S variant exhibits no detectable catalytic activity, and the C140S variant has a specific activity only 3% of that exhibited by the wild-type enzyme). These data provide convincing evidence that neither Cys140 nor Cys256 serve as ligands to the [4Fe−4S] cluster in PaAPR. The iron−sulfur cluster of the C256S variant of PaAPR appeared to be as stable as the cluster in the wild-type enzyme, as judged by the absence of detectable changes of the visible-region spectra over prolonged storage. In contrast, the iron−sulfur cluster in the C140S variant was considerably less stable, with the visible-region absorbance feature in the spectrum disappearing completely on storage at 5 °C over the period of a few hours (the time-course for cluster loss depended strongly on PaAPR concentration, with cluster loss being considerably more rapid at lower protein concentrations). In the presence of 2-mercaptoethanol, the iron−sulfur cluster in the C140S variant became much more stable, although it was still less stable than was the case for either the wild-type enzyme or for its C256S variant (the spectrum of the C140S variant, shown in Figure 2, which was obtained using a sample that had been stabilized by the addition of 2-mercaptoethanol, shows some significantly lower absorbance in the visible region than does the wild-type enzyme, arising from some cluster loss). Figure 3b shows that the resonance Raman spectrum of C256S variant of PaAPR is essentially identical to that of the wild-type enzyme, providing additional evidence that this cysteine residue does not serve as a ligand to the iron−sulfur cluster of the enzyme. The iron−sulfur cluster of the C140S variant was not sufficiently stable to allow resonance Raman spectra to be obtained.

In contrast to the results obtained with the C140S and C256S variants, changing any of the remaining PaAPR cysteines (i.e., Cys139, Cys228, or Cys231) to serine produced enzymes with no detectable absorbance in the visible region (not shown). Furthermore, unlike the C140S and C256S variants, the C139S, C228S, and C231S variants contained essentially no iron (Table 1). Although a full characterization of the properties of these cysteine/serine variants will be presented in a subsequent paper, it should be noted that all three of these variants (i.e., those in which Cys139, Cys228, or Cys231 have been replaced by serine) are completely inactive. While the C256S variant of PaAPR had iron and sulfide contents very similar to those of the wild-type enzyme, the C140S mutant contained significantly less iron and sulfide than did wild-type PaAPR (even in the presence of 2-mercaptoethanol), presumably due to the instability of the cluster in this variant (Table 1).

Gel-filtration experiments, carried out with the *L. minor* enzyme, suggest that it is a homodimer (*24*). Although we have not undertaken a detailed study of the subunit structure of PaAPR, it was of interest to determine whether either of the two PaAPR cysteines that do not serve as ligands to the iron−sulfur cluster might participate in intermolecular disulfide bonds between two identical PaAPR monomers. Thiol group quantitation of the native form of PaAPR that had been pretreated with oxidized DTT indicated the presence of 0.10 ± 0.10 mol of thiol per mol of enzyme DTT (redox titrations of PaAPR, shown next, suggest that treating samples of PaAPR in this manner completely oxidizes the two cysteines that do not serve as ligands to the iron−sulfur cluster to a disulfide). If Cys140 and Cys256 had been oxidized by the oxidized form of DTT to form a PaAPR intramolecular disulfide, then one would have expected that the oxidized enzyme would contain no thiol groups. Alternatively, if quantitative formation of an intermolecular disulfide between two identical PaPAR monomers had occurred, resulting in formation of a disulfide-linked dimer, one would have expected to find 1.0 thiol per PaAPR monomer. The experimental value of 0.10 thus suggests that, under the mildly oxidizing conditions established by addition of oxidized DTT, the two cysteines of PaAPR that do not serve as ligands to the iron−sulfur cluster are predominantly in the form of an intramolecular disulfide (for the sake of

simplicity, we have limited this analysis to these two cases and have not considered more complicated possibilities, i.e., those involving more than one disulfide per dimer or the presence of appreciable amounts of higher molecular mass oligomers). SDS−PAGE experiments, carried out in the absence of a reductant and using freshly prepared samples of PaAPR, do indeed reveal the presence of two Coomassie-staining bands (not shown), with molecular masses corresponding to those expected for PaAPR monomer and PaAPR dimer respectively (i.e., 35 and 70 kDa). Although the relative proportion of monomer and dimer in these SDS−PAGE experiments showed some variability from one preparation of enzyme to another, in all cases there was relatively little dimer seen, consistent with the DTNB analyses. Reducing SDS−PAGE experiments (i.e., experiments in which the samples were incubated with 2-mercaptoethanol prior to electrophoresis) showed only the $M_r = 35$ kDa PaAPR monomer and no dimer, indicating that the small amount of dimer present in the absence of 2-mercaptoethanol is likely to result from formation of a covalent disulfide bond. Thiol quantitation of samples of the cluster-free form of the enzyme that had been pretreated with oxidized DTT, to favor formation of a Cys140/Cys256 disulfide, indicated the presence of 3.19 ± 0.09 mol of thiol per mol of enzyme. This value provides additional support for the presence of three rather than four cysteine ligands to the cluster, if one assumes that none of the three cysteine residues was liberated on removal of the iron−sulfur cluster become involved in disulfide bond formation in the presence of oxidized DTT.

Figure 5A shows an oxidation−reduction titration of PaAPR, at pH 7.0, using the mBBr method described in the Materials and Methods to monitor the thiol content of the enzyme. The data give a good fit to the Nernst equation for a single two-electron redox couple with an E_m value of −292 mV. The E_m value and the $n = 2$ character of the titration curve, as well as the known specificity of mBBr for chemical modification of thiols (*19*, *20*), strongly suggest that the redox titration results can be attributed to a dithiol/disulfide redox couple. The average E_m value (six determinations) for this couple was −292 ± 8 mV at pH 7.0. Figure 5B shows the results of a redox titration of PaAPR, also carried out at pH 7.0, but using the intrinsic fluorescence of the enzyme to monitor its redox state. The data give a good fit to the Nernst equation for a single $n = 2$ component with $E_m = -306$ mV. The average E_m value (three determinations) for the redox titrations of tryptophan fluorescence at pH 7.0, −292 ± 18 mV, is identical, within the experimental uncertainties of the measurements, to that of the mBBr titrations, suggesting that the microenvironment for one or more tryptophan residues in PaAPR is altered when Cys140 and Cys256 become oxidized to a disulfide. No significant improvement in the fit to the Nernst equation was observed if an attempt was made to fit the data from either the mBBr titrations or the tryptophan fluorescence titrations to two $n = 2$ components instead of to a single $n = 2$ component. Redox titrations of PaAPR carried out at pH 8.5 (the pH optimum for enzymatic activity; ref *5*), instead of pH 7.0, gave an E_m value of −360 ± 10 mV (not shown). A process in which the reduction of a disulfide is accompanied by the uptake of two protons would be expected to have an E_m value at pH 8.5 that is ca. 90 mV more negative than the E_m value observed at pH 7.0. Thus, the fact that the experimentally

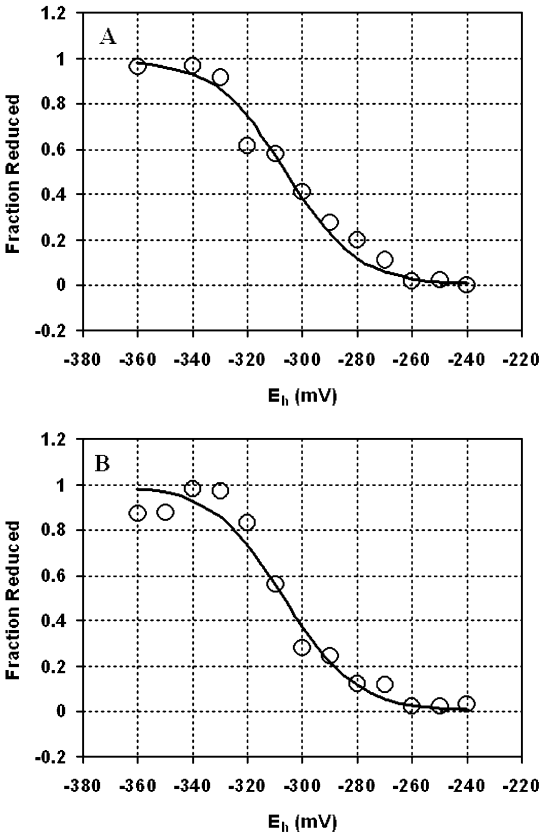

FIGURE 5: Oxidation−reduction titrations of wild-type PaAPR at pH 7.0. (A) Monobromobimane (mBBr) titration: wild-type PaAPR, at a concentration of 50 μg/mL, was titrated in 100 mM Hepes buffer (pH 7.0), at a total DTT concentration of 2.0 mM, with a redox equilibration time of 2.0 h. (B) Tryptophan titration: wild-type PaAPR, at a concentration of 5 μg/mL, was titrated in 100 mM Hepes buffer (pH 7.0), at a total DTT concentration of 2.0 mM, with a redox equilibration time of 2.0 h.

observed difference in the E_m values of PaAPR at these two pH values is only 66 mV indicates the presence of a pK_a for a group that couples disulfide reduction to proton uptake somewhere between pH 7.0 and 8.5.

It was not possible to carry out redox titrations or use DTNB to measure thiol content with the C140S variant of PaAPR because of the presence of 2-mercaptoethanol to stabilize this variant against loss of the iron−sulfur cluster. However, we have made such measurements with the C256S variant of the enzyme. The thiol content of this variant is 0.72 ± 0.07 as isolated, suggesting that while most of the enzyme is present as a monomer with the thiol of Cys140 accessible to DTNB, approximately 30% of the enzyme is present as a disulfide-linked dimer. Nonreducing SDS−PAGE analysis of the C256S variant of PaAPR confirmed the presence of dimer, which was eliminated by preincubation of the sample with reduced DTT (not shown) confirming that the dimer results from disulfide bond formation. Side-by-side redox titrations of wild-type PaAPR and its C256S variant showed that the amplitude of the E_h-dependent mBBr fluorescence observed in titrations of the C256S PaAPR variant is significantly smaller than that observed in titrations of the wild-type enzyme (i.e., between one-third and one-half), consistent with the results of DTNB analysis that show a smaller amount of DTT-reducible disulfide present in the C256S variant. Data from the mBBr titrations of the C256S variant of PaAPR gave a good fit to a single component, *n*

= 2 Nernst equation, with an E_m value of −305 mV at pH 7.0. Titrations of the intrinsic tryptophan fluorescence of the C256S variant at pH 7.0 also gave a good fit to the single-component, n =2 Nernst equation with an E_m value of −325 ± 14 mV. The 20 mV difference in E_m values obtained using the two different fluorescence indicators to monitor disulfide bond redox state in the C256S variant of PaAPR is greater than that observed for the wild-type enzyme, where the two methods gave identical E_m values. This may be due to the fact that the fluorescence amplitude is lower for the variant than for the wild-type. However, the two sets of E_m measurements for the C256S variant do agree with each other within the experimental uncertainties of the measurements, and the average E_m of −315 mV obtained for this intermolecular disulfide in a C256S PaAPR dimer is more negative than the E_m = −292 mV value obtained for the intramolecular disulfide present in wild-type PaAPR at pH 7.0 (see Figure 5) by ca. 30 mV, an amount that is just a bit greater than the experimental uncertainties in the measurements.

DISCUSSION

We have confirmed, by a variety of techniques, the report that PaAPR contains a single [4Fe−4S] cluster with three cysteine ligands, and we have provided the first evidence that ferricyanide can selectively remove the unique Fe to yield a $[3Fe-4S]^+$ cluster. In addition, we have provided convincing evidence that Cys139, Cys228, and Cys231 serve as the three cysteine ligands to the [4Fe−4S] cluster of PaAPR. Previously reported site-directed experiments, carried out with the *A. thaliana* enzyme AtAPR2, provided evidence that two of the five cysteines present in the plant enzyme (i.e., Cys129 and Cys248) are not involved in ligating the iron−sulfur cluster (*24*). Although the other C/S variants of AtAPR2 produced in this study were present entirely in inclusion bodies and could not be purified, Kopriva et al. concluded, by a process of elimination, that the remaining three cysteines (i.e., Cys128, Cys220, and Cys223) serve as the ligands to the iron−sulfur cluster in this *A. thaliana* APS reductase isoform (*24*). Amino acid sequence alignments of PaAPR and two higher plant enzymes (i.e., AtAPR2 and LmAPR) (Figure 1) indicate that all five of these cysteines are conserved when the two sequences are compared (*24*). Furthermore, a comparison of our data, obtained with PaAPR in the present study, with the data previously reported for AtAPR2 indicate that the same three cysteines serve as cluster ligands in both the plant and the bacterial enzymes.

Although we do not yet possess sufficient data to propose a unique mechanism for PaAPR, a model might well involve an initial reduction of a Cys140/Cys256 disulfide by reduced thioredoxin, followed by a subsequent reduction of APS by the reduced enzyme. Such a model would be consistent with kinetic data supporting a ping−pong mechanism for PaAPR with reduced thioredoxin as the first substrate (*5*) and is consistent with our observations that the C256S variant is completely inactive and that the specific activity of the C140S variant is only 3% that exhibited by the wild-type enzyme. The E_m value for the thioredoxin of *P. aeruginosa* that is likely to be the in vivo electron donor for the enzyme is not known. However, the E_m values for *E. coli* thioredoxin *1* and for spinach chloroplast thioredoxin *m* (*20*), two thioredoxins that are known to be good substrates for the enzyme (*5*), are sufficiently negative at pH 8.5 (the optimum pH for PaPAR activity), where E_m = −375 mV for *E. coli* thioredoxin 1 and E_m = −385 mV for spinach thioredoxin *m*, to reduce the PaPAR disulfide (E_m = −360 mV) in a thermodynamically favorable reaction. It should also be mentioned that although very small amounts of a disulfide-linked homodimer of the wild-type enzyme can be detected (and somewhat larger amounts of dimer can be detected in samples of the C256S variant), our data do not provide any evidence for a functional, disulfide-linked dimer operating during the normal catalytic cycle of the enzyme.

The role of the redox-inert $[4Fe-4S]^{2+}$ cluster in PaAPR remains elusive, but the observation that each of the individual cysteine to serine variants that contain no cluster are completely inactive suggests that the cluster does play an important role. A purely structural role seems unlikely in view of the lability of the cluster and the presence of a unique noncysteinyl-ligated Fe site. In addition, the evidence for a disulfide between the active-site cysteine, C256, and C140, which is adjacent to one of the cluster ligating cysteines, C139, positions the cluster in close proximity to the substrate binding site. Interestingly, the close correspondence in the RR spectra of PaAPR in the absence and presence of DTT indicates that the formation of a disulfide between C256 and C140 does not significantly perturb the immediate environment of the $[4Fe-4S]^{2+}$ cluster. However, C140 does appear to play a role in stabilizing the cluster as evidenced by the increased lability of the cluster in the C140S variant and in oxidized samples in which the disulfide is intact. By analogy with aconitase, it is tempting to speculate that the cluster might play a role in binding and activating the substrate. The sensitivity of the RR spectrum of $[4Fe-4S]^{2+}$ centers to ligand binding at a unique site and to small changes in the cluster environment (*26*, *28*, *32*) therefore provides a means of addressing the possibility that the cluster plays a role in substrate activation. Such experiments are currently in progress.

ACKNOWLEDGMENT

The authors thank Dr. Susan Kleis-SanFrancisco for sequencing wild-type PaAPR and its proteolytic degradation product.

REFERENCES

1. Kredich, N. M. (1996) Biosynthesis of cysteine, in *Escherichia coli and Salmonella typhimurium* in *Cellular and Molecular Biology* (Neidhardt, F. C., Curtiss, R., Ingraham, J. L., Lin, E. C. C., Low, K. B., Magasanik, B., Reznikoff, W. S., Riley, M., Schaechter, M., and Umberger, E., Eds) pp 514−527, ASM Press, Washington D.C.
2. Setya, A., Murillo, M., and Leustek, T. (1996) Sulfate reduction in higher plants: molecular evidence for a novel 5′-adenylyl sulfate reductase, *Proc. Natl. Acad. Sci. U.S.A. 93*, 13383−13388.
3. Gutierrez-Marcos, J. F., Roberts, M. A., Campbell, E. I., and Wray, J. L. (1996) Three members of a novel small gene-family from *Arabidopsis thaliana* able to complement functionally an *Escherichia coli* mutant defective in PAPS reductase activity encode proteins with a thioredoxin-like domain and APS reductase activity, *Proc. Natl. Acad. Sci. U.S.A. 93*, 13377−13382.
4. Abola, A. P., Willits, M. G., Wang, R. C., and Long, S. R. (1999) Reduction of adenosine-5′-phosphosulfate instead of 3′-phosphoadenosine-5′-phosphosulfate in cysteine biosynthesis by *Rhizobium meliloti* and other members of the family *Rhizobiaceae*, *J. Bacteriol. 181*, 5280−5287.
5. Bick, J. A., Dennis, J. J., Zylstra, G. J., Nowack, J., and Leustek, T. (2000) Identification of a new class of 5′-adenlyyl sulfate (APS) reductase from sulfate-assimilating bacteria, *J. Bacteriol. 182*, 135−142.

6. Neumann, S., Wynen, A., Trüper, H. G., and Dahl, C. (2000) Characterization of the cys gene locus from Allochromatium vinosum indicates an unusual sulfate assimilation pathway, *Mol. Biol. Rep. 27*, 27−33.
7. Williams, S. J., Senaratne, R. H., Mougous, J. D., and Riley, L. W., and Bertozzi, C. R. (2002) 5′-Adenosinephosphosulfate lies at a metabolic branch point in mycobacteria, *J. Biol. Chem. 277*, 32606−32615.
8. Kopriva, S., Buchert, T., Fritz, G., Suter, M., Benda, R., Schunemann, V., Koprivova, A., Schurmann, P., Trautwein, A. X., Kroneck, P. M., and Brunold, C. (2002) The presence of an iron−sulfur cluster in adenosine 5′-phosphosulfate reductase separates organisms utilizing adenosine 5′-phosphosulfate and phosphoadenosine 5′-phosphosulfate for sulfate assimilation, *J. Biol. Chem. 277*, 21786−21791.
9. Berendt, U., Haverkamp, T., Prior, A., and Schwenn, J. D. (1995) Reaction mechanism of thioredoxin: 3′-phospho-adenylyl sulfate reductase investigated by site-directed mutagenesis, *Eur. J. Biochem. 233*, 347−356.
10. Weber, M., Suter, M., Brunold, C., and Kopriva, S. (2000) Sulfate assimilation in higher plants characterization of a stable intermediate in the adenosine 5′-phosphosulfate reductase reaction, *Eur. J. Biochem. 267*, 3647−3653.
11. Berndt, C., Lillig, C. H., Wollenberg, M., Bill, E., Mansilla, M. C., de Mendoza, D., Seidler, A., and Schwenn, J. D. (2004) Characterization and reconstitution of a 4Fe−4S adenylyl sulfate/phosphoadenylyl sulfate reductase from *Bacillus subtilis*, *J. Biol. Chem. 279*, 7850−7855.
12. Savage, H., Montoya, G., Svensson, C., Schwenn, J. D., and Sinning I. (1997) Crystal structure of phosphoadenylyl sulphate (PAPS) reductase: a new family of adenine nucleotide alpha hydrolases, *Structure 5*, 895−906.
13. Bick, J. A., Åslund, F., Chen, Y., and Leustek T. (1998) Glutaredoxin function for the carboxyl terminal domain of the plant-type 5′-adenylyl sulfate (APS) reductase, *Proc. Natl. Acad. Sci. U.S.A. 95*, 8404−8409.
14. Sambrook, J., Fritsch, E., and Maniatis, T. (1989) *Molecular cloning: a laboratory manual*, 2nd ed., Cold Spring Harbor Laboratory Press, Cold Spring Harbor, NY.
15. Balmer, Y., Stritt-Etter, A. L., Hirasawa, M., Jacquot, J.-P., Keryer, E., Knaff, D. B., and Schurmann, P. (2001) Oxidation−reduction and activation properties of chloroplast fructose 1,6-bisphosphatase with mutated regulatory site, *Biochemistry. 40*, 15444−15450.
16. Habeeb, A. F. S. A. (1972) Reaction of protein sulfhydryl groups with Ellman's reagent. *Methods Enzymol. 25*, 457−464.
17. Massey, V. (1957) Studies on succinic dehydrogenase: vii. valency state of the iron in beef heart succinic dehydrogenase, *J. Biol. Chem. 229*, 763−770.
18. King, T. E., and Morris, R. O. (1967) Determination of acid-labile sulfide and sulfhydryl groups, *Methods Enzymol. 10*, 634−641.
19. Krimm, I., Lemaire, S. D., Ruelland, E., Miginiac-Maslow, M., Jacquot, J.-P., Hirasawa, M., Knaff, D. B., and Lancelin, J.-M. (1998) *Eur. J. Biochem. 255*, 185−195.
20. Hirasawa, M., Schürmann, P., Jacquot, J.-P., Manieri, W., Jacquot, P., Keryer, E., Hartman, F. C., and Knaff, D. B. (1999) Oxidation−Reduction Properties of Chloroplast Thioredoxins, Ferredoxin: Thioredoxin Reductase and Thioredoxin f-Regulated Enzymes, *Biochemistry 38*, 5200−5205.
21. Drozdzewski, P. M., and Johnson, M. K. (1988) A simple anaerobic cell for low-temperature Raman spectroscopy, *Appl. Spectrosc. 42*, 1575−1577.
22. Johnson, M. K. (1988) Variable temperature magnetic circular dichroism studies of metalloproteins, in *ACS Symposium Series 372*: *Metal Clusters in Proteins* (Que, L., Jr., Ed.) pp 326−342, American Chemical Society, Washington, D.C.
23. Thomson, A. J., Cheesman, M. R., and George, S. J. (1993) Variable-temperature magnetic circular dichroism, *Methods Enzymol. 226*, 199−232.
24. Kopriva, S., Buchert, T., Fritz, G., Suter, M., Weber, M., Benda, R., Schaller, J., Feller, U., Schurmann, P., Schunemann, V., Trautwein, A. X., Kroneck, P. M., and Brunold, C. (2001) Plant adenosine 5′-phosphosulfate reductase is a novel iron−sulfur protein, *J. Biol Chem. 276*, 42881−42886.
25. Czernuszewicz, R. S., Macor, K. A., Johnson, M. K., Gewirth, A., and Spiro, T. G. (1987) Vibrational mode structure and symmetry in proteins and analogues containing Fe_4S_4 clusters: Resonance Raman evidence for different degrees of distortion in HiPIP and ferredoxin, *J. Am. Chem. Soc. 109*, 7178−7187.
26. Kilpatrick, L. K., Kennedy, M. C., Beinert, H., Czernuszewicz, R. S., Qui, D., and Spiro, T. G. (1994) Cluster structure and H-bonding in native, substrate-bound, and 3Fe forms of aconitase as determined by resonance Raman spectroscopy, *J. Am. Chem. Soc. 116*, 4053−4060.
27. Conover, R. C., Kowal, A. T., Fu, W., Park, J.-B., Aono, S., Adams, M. W. W., and Johnson, M. K. (1990) Spectroscopic characterization of the novel iron−sulfur cluster in *Pyrococcus furiosus* ferredoxin, *J. Biol. Chem. 265*, 8533−8541.
28. Brereton, P. S., Duderstadt, R. E., Staples, C. R., Johnson, M. K., and Adams, M. W. W. (1999) Effect of serinate ligation at each of the iron sites of the $[Fe_4S_4]$ cluster of *Pyrococcus furiosus* ferredoxin on the redox, spectroscopic, and biological properties, *Biochemistry 38*, 10594−10605.
29. Cosper, M. M., Krebs, B., Hernandez, H., Jameson, G., Eidsness, M. K., Huynh, B. H., and Johnson, M. K. (2004) Characterization of the cofactor content of *Escherichia coli* biotin synthase, *Biochemistry 43*, 2007−2021.
30. Johnson, M. K., Duderstadt, R. E., and Duin, E. C. (1999) Biological and Synthetic $[Fe_3S_4]$ Clusters, *Adv. Inorg. Chem. 47*, 1−82.
31. Beinert, H., Kennedy, M. C., and Stout, C. D. (1996) Aconitase as iron−sulfur protein, enzyme, and iron-regulatory protein, *Chem. Rev. 96*, 2335−2373.
32. Cosper, M. M., Jameson, G. N. L., Davydov, R., Eidsness, M. K., Hoffman, B. M., Huynh, B. H., and Johnson, M. K. (2002) The $[4Fe-4S]^{2+}$ cluster in reconstituted biotin synthase binds *S*-adenosylmethionine, *J. Am. Chem. Soc. 124*, 14006−14007.

BI048811T